International Journal of Fracture **129:** 279–308, 2004.

Modeling of fatigue crack closure in inclined and deflected cracks

S. KIBEY[1], H. SEHITOGLU[1,*] and D.A. PECKNOLD[2]
[1] *University of Illinois, Department of Mechanical and Industrial Engineering, 1206, W. Green St., Urbana, IL 61801, USA*
[2] *University of Illinois, Department of Civil and Environmental Engineering, 205 N. Mathews St., Urbana, IL 61801, USA*
[*] *Author for correspondence (E-mail: huseyin@uiuc.edu)*

Received 16 October 2003; accepted in revised form 7 May 2004

Abstract. A 2-dimensional, elastic-plastic finite element model has been developed to simulate plasticity induced crack closure in slanted and deflected cracks growing outside the small scale yielding (SSY) regime. The finite element model allows for contact between deformable surfaces to capture the complex contact interaction between the crack faces. Coulomb's friction law has been used to model friction between the crack faces and has been incorporated in the finite element model. This paper examines the mode I and mode II behavior of slanted cracks subjected to remote mode I, constant amplitude cyclic loading. Two possible types of mode II crack face interaction have been identified: (a) complete slip in mode II before mode I opening and, (b) mode I crack opening before the crack faces undergo mode II displacements. Both types of interactions were observed in slanted cracks. The finite element study also reveals a clear dependence of mode I and mode II crack opening levels for a slanted crack on R ratio and maximum stress, S_{max}/σ_0. The crack opening levels for a slanted crack are found to be significantly higher than the stable opening values for a straight crack growing in pure mode I. The mode I and mode II crack opening levels are also found to depend on the friction between the crack faces. A four-fold increase in friction coefficient resulted in almost 50% increase in normalized mode I and mode II opening values. This paper also describes the effect of crack deflection on closure. Deflection of a fatigue crack from 45° inclination to pure mode I caused a decrease in mode I opening level, but, an increase in mode II opening level. This difference in opening behavior is attributed to the transition of the nature of crack interaction from 'complete slip before opening' to 'opening in mode I before mode II shear offset'. Final stable opening levels for a deflected crack are found to be close to the stable value for straight cracks.

Key words: Fatigue, fracture, crack closure, finite elements, slanted cracks, deflected cracks, contact mechanics

Nomenclature

Δa	= Increment in crack length, element size
CCT	= Center cracked tension specimen
da/dN	= Crack growth rate
E	= Elastic modulus
H	= Hardening modulus
J	= J Integral
ΔK_{eff}	= Effective stress intensity range
L	= Crack length in SENT specimen
L^*	= Minimum slanted crack length required for stability of mode I opening level

L_0	=	Initial crack length in SENT specimen
p_c	=	Contact pressure
PICC	=	Plasticity induced crack closure
R	=	Load ratio
RICC	=	Roughness induced crack closure
S	=	Applied stress
SENT	=	Single edge notched specimen
S_{max}	=	Maximum applied stress level
S_{min}	=	Minimum applied stress level
$S_{op\ I}$	=	Mode I crack opening level
$S_{op\ II}$	=	Mode II crack opening level
$U_{I,lower}$	=	Normal (mode I) displacement of the lower crack face from its initial position
$U_{I,upper}$	=	Normal (mode I) displacement of the upper crack face from its initial position
$U_{II,lower}$	=	Transverse (mode II) displacement of the lower crack face from its initial position
$U_{II,upper}$	=	Transverse (mode II) displacement of the upper crack face from its initial position
W	=	Width of the SENT specimen
σ_0	=	Uniaxial yield strength
σ_n	=	Stress component normal to the fatigue crack faces
ε_n	=	Strain component normal to the fatigue crack faces
ν	=	Poisson's ratio
ΔU_I		= Mode I crack opening displacement of fatigue crack
$\Delta U_{I\,max,st}$	=	Mode I crack opening displacement of stationary crack at maximum load
ΔU_{II}	=	Mode II crack opening displacement of fatigue crack
$\Delta U_{II\,max,st}$	=	Mode II crack opening displacement of stationary crack at maximum load
δ_{resid}	=	Residual plastic deformation along the wake
μ	=	Coefficient of friction between the crack faces
θ	=	Orientation of inclined crack relative to horizontal
τ	=	Shear stress along the crack flanks
τ_0	=	Yield strength in shear

1. Introduction

It has been well established that crack closure is an important phenomenon in fatigue crack growth and significantly affects the fatigue crack growth rates. First discovered by Elber (1970, 1971) crack closure has been extensively studied in the past three decades. The crack growth relationship based on closure can be written as

$$\mathrm{d}a/\mathrm{d}N = C\,(\Delta K_{\mathrm{eff}})^m \tag{1}$$

where, C and m are empirical constants. ΔK_{eff} is the effective stress intensity range during which the crack is open. The effective stress intensity range is dependent on the extent of closure occurring during fatigue crack propagation. The concept of crack closure has been useful in explaining many experimentally observed behaviors such as stress ratio effects, effect of notches, constraint effects (plane stress, plane strain), overload effects, variable amplitude loading, stress biaxiality effects etc, behavior of short cracks etc.

Over the past 30 years, numerous finite element models have been proposed to explain the phenomenon of crack closure. The use of finite elements in crack closure studies was undertaken for the first time by Ohji, Ogura and Ohkubo (1974). They presented crack closure analysis in fatigue cracks growing from notches under variable amplitude and biaxial loadings. Newman (1976) developed a finite element model to predict crack closure in fatigue cracks under constant amplitude loading and later modified it to include effects of variable amplitude loading (Newman, 1981). Shiratori et al. (1977) reported stress, strain and displacement analysis to explain closure effects in fatigue cracks under constant amplitude loading. Budiansky and Hutchinson (1978) developed an analytical model to support the existence of crack closure in fatigue crack growth phenomenon. Blom and Holm (1985) published closure results for different stress ratios in CT specimens under plane stress and plane strain conditions. Fleck (1986) and later, Fleck and Newman (1988) considered the effect of plane stress and plane strain conditions on crack closure. Sehitoglu et al. (1990, 1992) followed this work by conducting a detailed closure study on constraint effects (plane stress, plane strain). Lalor and Sehitoglu (1988) developed an elastic-plastic code to model plasticity induced crack closure in fatigue cracks growing out of a notch. McClung and Sehitoglu (1989) carried out a systematic study of modeling closure using finite elements and laid basic criteria for mesh sufficiency and determined the effect of various parameters such as stress level, R-ratio, H/E ratio, constraint effects, and notch effects etc on crack closure.

The fatigue crack closure models discussed above fundamentally assume plasticity induced crack closure (PICC) as the only mechanism of closure. These models ignore the role of other known closure mechanisms like roughness induced crack closure (RICC), oxide induced crack closure and transformation induced crack closure. RICC is the dominant closure mechanism in cracks growing in near threshold regime in planar slip materials and coarse-grained materials. Beevers et al. (1979) proposed a simple physically based model to account for roughness effects. Suresh and Ritchie (1982) developed a geometric model to describe roughness induced crack closure in fatigue cracks. Tschegg (1983) used the term 'sliding mode crack closure' (SMCC) to describe the effect of reduction in nominal stress intensity factor due to friction between the crack faces. Tong, Yates and Brown (1995) developed a model for SMCC to quantify the closure in cracks subjected to cyclic mode II loading conditions. Utilizing the concept of SMCC, they were able to explain near threshold behavior of fatigue cracks growing under mixed mode conditions (Brown et al. 1994). Llorca (1992) used finite difference method to analyze roughness induced crack closure due to corrugated crack faces. This study, however,

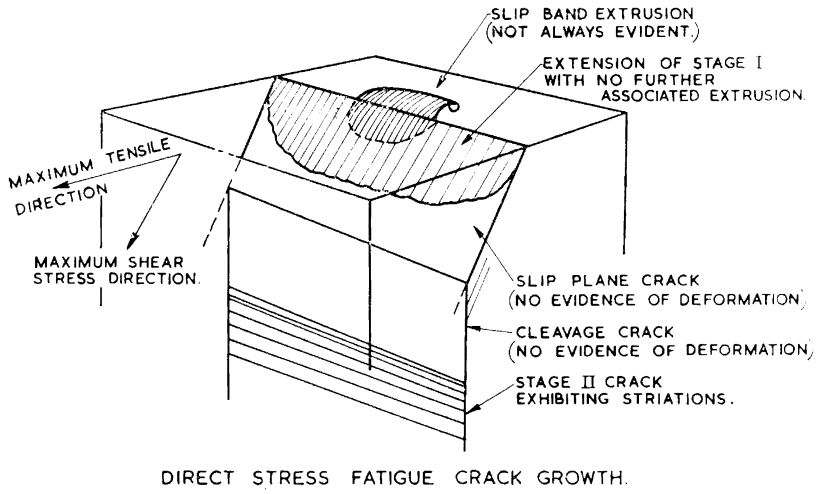

Figure 1. Stage I and stage II fatigue crack growth (Forsyth, 1963).

did not consider the effect of friction between the crack faces or the effect of plasticity induced crack closure on fatigue crack behavior. Sehitoglu and Garcia (1995) proposed a model predicting and quantifying roughness induced crack closure. Sehitoglu, Gall and Kadioglu (1996) investigated closure occurring in micro structurally small cracks within a grain using crystal plasticity theory. Friction has also been modeled at macroscopic level in case of partially or completely closed cracks. Comninou and Dundurs (1979) developed an analytical model for stick-slip behavior of partially closed cracks. Mendelsohn and Wang (1988) examined the effect of frictional coefficient on mode II behavior of finite length cracks subjected to remote compression and pure shear.

Much of the research done in the past on fatigue crack closure has been limited to planar crack fronts. However, in practice, a fatigue crack is likely to deviate from its original path and propagate as a non-planar crack. It is known that fatigue cracks growth process occurs in two distinct stages designated as stage I and stage II. Stage I refers to growth of slip band cracks formed along the extruded slip bands. These slip band cracks propagate along planes of maximum shear under combined mode I and mode II conditions, but, actively growing cracks are seen only after the slip band cracks turn from maximum shear stress direction towards maximum tensile stress direction and essentially start growing in mode I (Forsyth, 1963) (see Figure 1). Crack growth along the maximum tensile stress direction is referred to as stage II fracture which is characterized by formation of striations.

In the literature reviewed so far, almost all results were reported for pure mode I conditions, except for the work of Nakagaki and Atluri (1980) and to some extent the research of McClung and Sehitoglu (1989). Nakagaki and Atluri (1980) were probably the first to publish elastic-plastic finite element analysis of fatigue cracks under mixed mode loading conditions. They used singular element to capture crack tip singularity and considered both constant amplitude and variable amplitude loading for mode I and only constant amplitude loading for mode II .They were able to report the crack acceleration and retardation effects under general spectrum loading using crack closure. Recently, Parry et al. (2000) reported a finite element model for a continuously deflecting fatigue crack with local mixed mode behavior. However, their work focuses on the combined effects of PICC and RICC only on mode I opening levels. Limited attention was placed on mode II effects. The recent work of Wei and James (2002) reported a

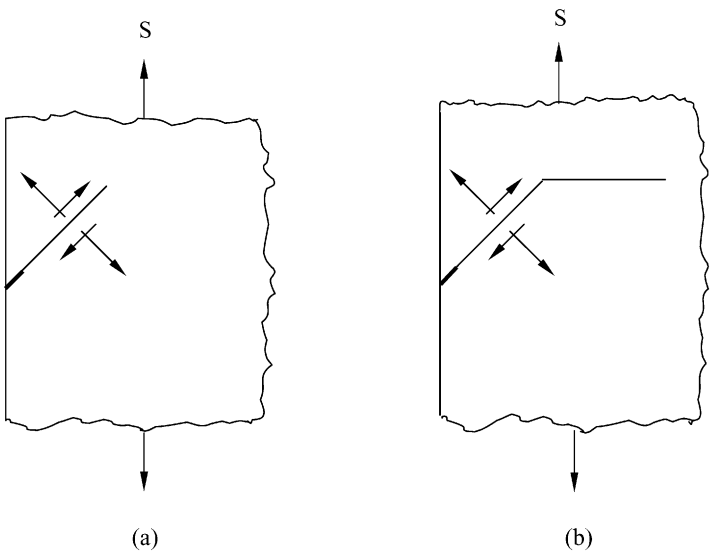

Figure 2. (a) Slanted crack (b) Deflected crack.

finite element model of PICC in inclined and kinked cracks. They reported the effects of crack deflection, crack orientation and friction between crack faces on mode I crack opening levels, but, overlooked the role of crack closure in mode II.

A few analytical models for mixed-mode crack closure are also available. Alwar and Thiagarajan (1986) examined the effect of closure on crack initiation direction in case of angled cracks. Qian and Fatemi (1996) have summarized the experimental, analytical and numerical efforts in modeling mixed-mode crack closure.

The present research is a step further in finite element modeling of closure in slanted and deflected fatigue cracks. The finite element model is capable of incorporating the role of plasticity, contact interaction of the crack faces, frictional effects and crack path deflection on crack closure. This research addresses some of the issues involved in modeling crack closure in non-planar fatigue cracks which will be geometrically similar to the crack depicted in Figure 2.

2. Purpose and scope of this research

This paper presents a 2-D elastic-plastic finite element model to analyze fatigue crack closure in cracks which deviate from their original path. The phenomenon of closure in such cracks will involve not only plasticity induced crack closure mechanism but also the relative sliding between the crack faces and the frictional effects arising out of such relative sliding. Thus, it becomes essential to incorporate the effect of both plasticity and frictional nonlinearities on closure behavior of a fatigue crack. Fatigue cracks, in general, can start growing in a particular direction and then deflect to grow in a different direction. Such cracks have been termed as 'deflected cracks' in this research. It is also possible that some fatigue cracks may grow at an angle relative to the remote load. The term 'slanted cracks' or 'inclined cracks' will be used to describe these cracks. Figure 2 illustrates a slanted and a deflected crack which are subjected to mode I remote loading but exhibit local mixed-mode behavior.

The extent of closure occurring in fatigue cracks can be quantified with ΔK_{eff} and the dependence of ΔK_{eff} on various parameters can be expressed as:

$$\Delta K_{\text{eff}} = f\left(\frac{S_{\max}}{\sigma_0}, R, \frac{H}{E}, \frac{\sigma}{\sigma_H}, \mu, a, \text{Geometry, Microstructure, constraint}\right) \tag{2}$$

In this study, we investigate the effect of applied stress S_{max}/σ_0 on the closure behavior of both slanted and deflected fatigue cracks. The term geometry in equation (2) implies both geometry of the specimen (SENT, CT etc.) and the geometry of the crack (crack orientation and crack path). Here, we specifically address the latter i.e. the effect of crack orientation and crack path on crack closure. This is achieved by investigating the crack closure behavior of slanted and deflected cracks with certain predetermined orientations. The R-ratio effect is investigated by considering two different R ratios: $R = 0$ and $R = -1$. Further, effect of friction on crack closure is incorporated in the analysis by accounting for friction between the crack faces in the finite element model.

3. Limitations of available finite element models

Since the pioneering work of Ohji, Ogura and Ohkubo (1974) and Newman (1976) in modeling crack closure using finite elements, a wide variety of two and three dimensional finite element models involving different crack configurations and element types have been reported by researchers. Ohji et al. (1974), Newman (1976), Fleck and Newman (1988) and several other researchers used triangular elements in both plane stress and plane strain. Nakagaki and Atluri (1979, 1980) used singular elements to capture HRR singularity at the crack tip. Chermahini et al. (1988) developed a threedimensional elastic-plastic finite element model using 8 node hexahedron elements. Lalor and Sehitoglu (1988), McClung and Sehitoglu (1989) and later Sehitoglu and Sun (1990, 1992) used 4 node isoparametric elements in their finite element models. The work of McClung and Sehitoglu (1989) was the first to critically examine issues of mesh design, mesh refinement and crack advancing scheme employed in such finite element models. They laid down several criteria of mesh sufficiency and crack advancing scheme to obtain reliable finite element results. Recently, Solanki et al. (2003) have examined mesh refinement effects in modeling PICC using finite elements. Their recommendations are in agreement with those of McClung and Sehitoglu (1989).

It should be noted that bulk of the finite element work in modeling crack closure has been performed on straight cracks using symmetry conditions to reduce the model size and to overcome difficulty in modeling crack face contact. Spring elements were used by most researchers [e.g. Newman (1976), Fleck and Newman (1988), McClung and Sehitoglu (1989)] to model crack closure. Spring stiffness was set to a very high value when the COD reduced to zero and when the stress state behind the crack changed from compressive to tensile, the stiffness was set to zero to allow the crack to open. Thus, rigid contact was modeled between the crack faces using spring elements. Since, these elasticplastic finite element models assumed crack plane symmetry they cannot be extended to model crack deflection and therefore, the closure resulting from it.

Limited attempts have been made to model contact interaction between the crack faces during closure without using symmetry. Parry et al. (2000) modeled PICC and RICC in continuously deflecting cracks, but, they followed the work of Newman (1976) to model contact using spring elements (rigid contact). Further, they did not consider the effect of

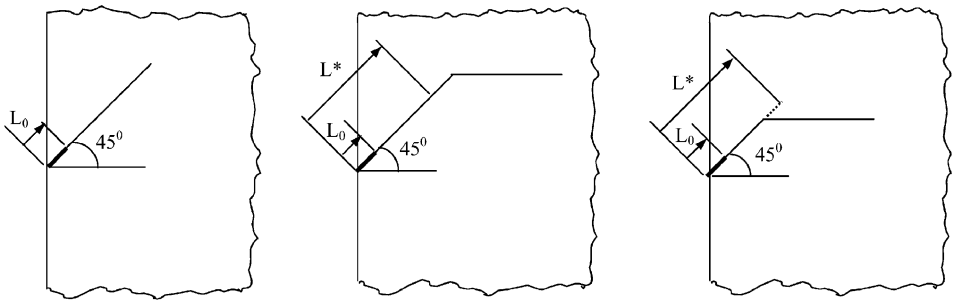

Figure 3. (a) Geometry 1: slanted crack (b) Geometry 2: crack deflection after stabilization (c) Geometry 3: crack deflection before stabilization. (L^* denotes the 'stabilization' crack length).

friction during contact of crack surfaces. Wei and James (2002) used contact capability in commercially available software ANSYS to model PICC in inclined and kinked cracks. Their analysis, however, does not consider the mode II behavior in inclined and kinked cracks. The finite element model used in this research overcomes the limitations of the models described above and presents a more versatile approach to modeling PICC in fatigue cracks.

4. Finite element model

A two dimensional elastic-plastic finite element model has been developed using commercial code ABAQUS (2000) with provision to grow a slanted or deflected crack in the specimen. The material is modeled to follow a bilinear stress-strain relationship. It exhibits linear elasticity below its initial yield strength $\sigma_0 = 480$ MPa. The Young's modulus is assumed to be $E = 200$ GPa and Poisson's ratio is assumed to be $\nu = 0.30$. The material follows a Mises yield criterion with linear kinematic hardening to capture Bauschinger effect associated with reversed yielding. The hardening modulus H is assumed to be constant, equal to $0.01E$, which is typical of low hardening steels and several aluminum alloys. Plane stress conditions have been assumed.

Before describing the details of mesh development, crack advance scheme, mesh refinement and contact modeling, we outline the specimen geometries investigated in this research. As mentioned before, an important objective of this research is to examine the effect of crack orientation and crack path on plasticity induced crack closure. To this end, following specimen geometries were considered:

a. Geometry 1: A SENT specimen with an initial edge crack inclined at an angle of 45° to the direction of applied loading in mode I. The fatigue crack is allowed to propagate along the 45° direction without deviating from its path. This geometry facilitates determination of stable opening levels for a fatigue crack oriented at 45° (Figure 3a).
b. Geometry 2: A SENT specimen with an edge crack inclined at an angle of 45° to the direction of applied loading which is initially allowed to propagate in the 45° direction long enough to attain stable opening levels and subsequently allowed to deflect and grow perpendicular to the mode I loading (Figure 3b). In other words, geometry 2 depicts the case of crack 'deflection after stabilization'. The length of the slanted part of the crack exceed the minimum required crack length to attain stabilization (denoted by L^*).

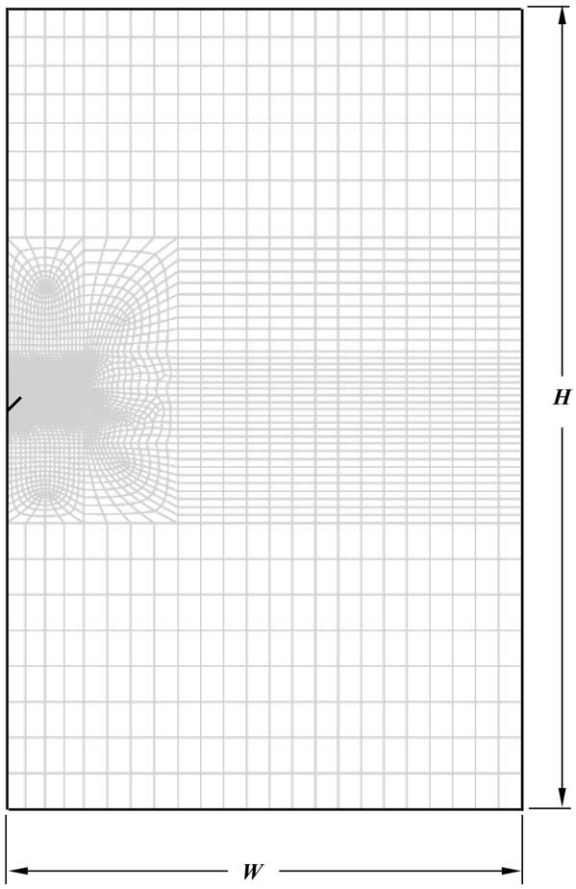

Figure 4. Typical finite element mesh for the SENT specimen with an angled crack. $H = 70$ mm, $W = 50$ mm.

c. Geometry 3: A SENT specimen with an edge crack inclined at an angle of 45° to the direction of applied loading which is initially allowed to propagate in the 45° direction. However, the crack is allowed to deflect and grow perpendicular to the applied loading before stable opening levels are attained (Figure 3c). This then is the case of 'deflection before stabilization'. In this case, the length of the slanted part of the crack is less than L^*.

While geometry 1 helps to determine the effect of crack orientation on mode I and mode II opening levels, geometries 2 and 3 provide insight into the effect of crack path on crack opening levels.

5. Finite element mesh

Figure 4 shows a representative mesh for the SENT specimen with an initial angled crack. The specimen dimensions were $H = 70$, $W = 50$ and initial crack length, $L_0 = 0.2828$. Figures 5, 6 and 7 shows the near tip finite element meshes for the three crack geometries described in the previous section. Four node isoparametric elements (Q4) were used to descritize the geometries. The use of Q4 elements permits linear stress and strain distributions in the finite element model. The mesh was particularly refined in the region surrounding the fatigue crack

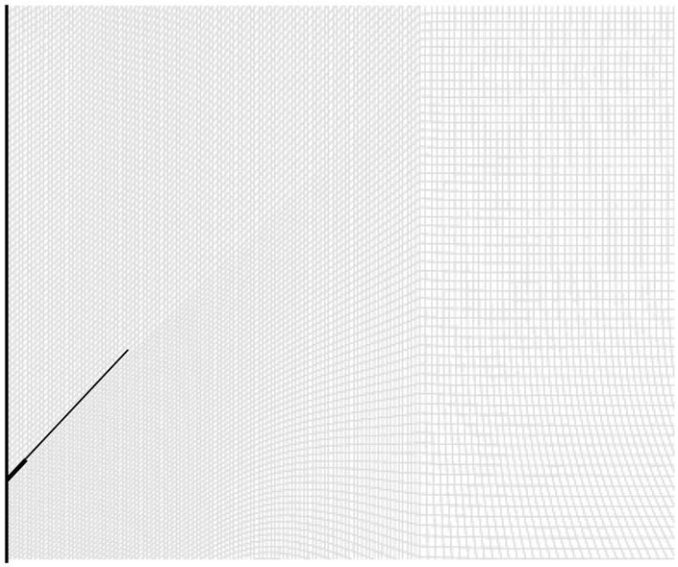

Figure 5. Near tip finite element mesh for geometry 1 (slanted crack, no deflection).

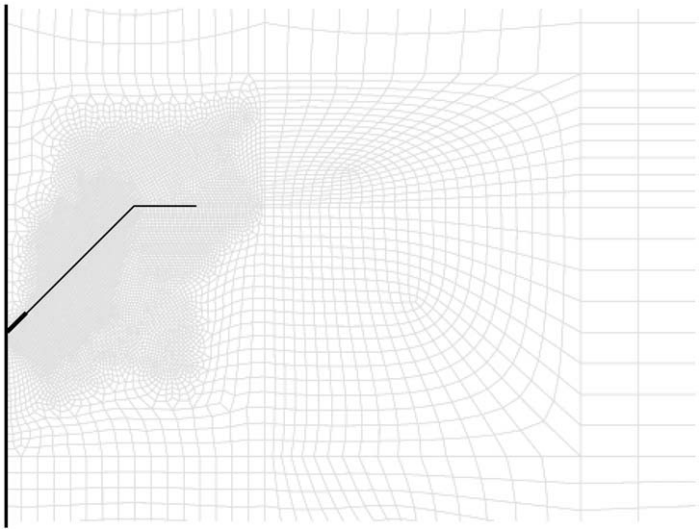

Figure 6. Near tip finite element mesh for geometry 2 (Deflection after stabilization).

to capture near tip plastic deformations. Note that symmetry does not exist in any of the three geometries and consequently, entire specimen needs to be discretized in each case. In order to obtain reliable finite element results, it is essential that the FE mesh should be able to capture both forward and reversed plastic zones, since reversed plasticity plays a crucial role in the crack closure phenomenon. According to McClung and Sehitoglu (1989), the mesh sufficiency criteria are given by:

$$\begin{aligned} \frac{\Delta a}{r_p} &\leqslant 0.1 \qquad \text{for} \quad R = 0 \\ \frac{\Delta a}{r_p} &\leqslant 0.15 \qquad \text{for} \quad R = -1 \end{aligned} \tag{3}$$

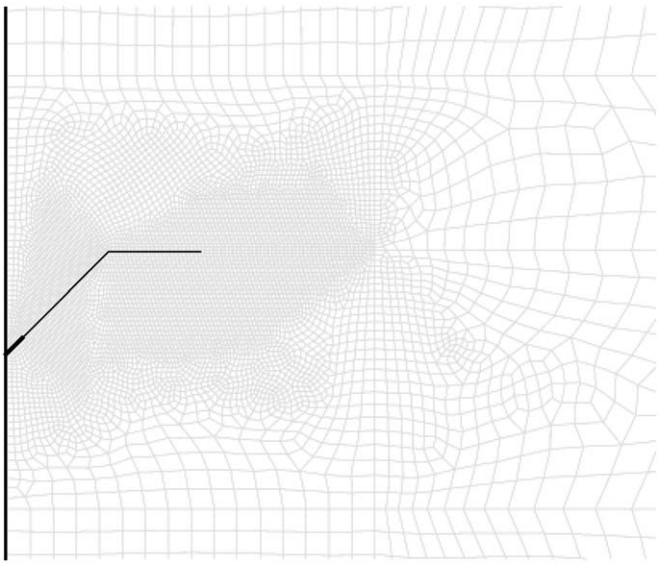

Figure 7. Near tip finite element mesh for geometry 3 (Deflection before stabilization).

All the finite element meshes employed in this research satisfy the above mesh sufficiency criteria. Typical size of an element (and hence the crack growth increment per cycle) along the crack line corresponds to $a/W = 0.0014$. The number of elements in such a mesh varied from 30000 to 50000 depending on the crack geometry.

In addition to correct modeling of plastic deformations, it is essential to model the contact interactions between the crack faces as the fatigue crack propagates. Surfacebased contact elements available in ABAQUS (2000) have been used to define the crack faces as deformable contacting surfaces. Small sliding has been allowed to capture the relative motion between the crack faces when they are in contact. It should be noted that an acceptable degree of mesh refinement is required along the contacting faces to model the contact mechanics correctly. As no quantitative criteria are currently available to determine mesh sufficiency for contact modeling, the authors conducted several simulations to verify the contact model and validate the meshes employed in fatigue simulations. Consequently, the mesh sizes mentioned earlier meet mesh sufficiency requirements with regard to plasticity as well as contact mechanics.

6. Crack advance scheme

Several crack tip node release schemes have been suggested in the finite element modeling of crack closure. Newman (1976), Fleck and Newman (1986), Blom and Holm (1986) and Chermahini et al. (1988) released the crack tip node at maximum load and allowed for the redistribution of the loads before beginning the unloading of the specimen. Ohji (1977) and Nakamura et al. (1983) released the crack tip node at minimum load in the fatigue cycle. Nakagaki and Atluri (1979, 1980) found that crack opening and closure levels were sensitive to the load at which crack extension was carried out. In their research, they calibrated the crack extension load in a cycle such that the computed opening levels were in good agreement with the experimental values. Lalor and Sehitoglu (1986) released the crack tip node immediately after the maximum load during the first increment of unloading. McClung and Sehitoglu (1989) investigated the effect of all the above schemes and concluded that all of them gave similar

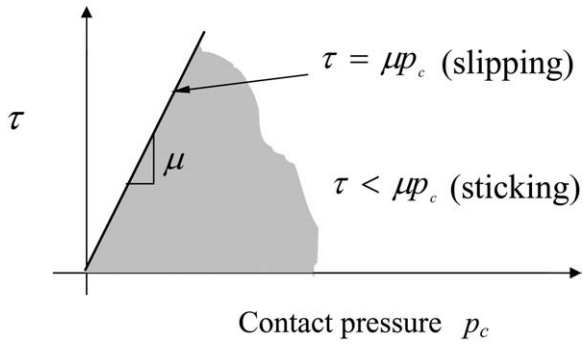

Figure 8. Coulomb's friction model.

results. They further pointed out that release of crack tip node immediately after maximum load gave the most consistent results. Hence, in this research, crack tip node has been released immediately after the maximum load during the first increment of unloading. In almost all simulations, the crack has been extended by one element size in each fatigue cycle. In some simulations, three to five nodes were released immediately after the maximum load to reduce computational time. It is believed that this scheme did not affect the crack opening levels significantly since the mesh was sufficiently fine. Note that the closure behavior of the first node behind the crack tip has been found to be anomalous. Since, crack tip node is released immediately after the maximum load, during unloading this node closes significantly prior to the point at which rest of the crack starts closing. Hence, it is essential to carefully define the crack opening and closure levels to obtain meaningful and error free results. The definitions for opening levels used in this research are summarized in a later section.

7. Friction model

The friction between the contacting crack surfaces is modeled using simple Coulomb's friction model which can be summarized as

$$\begin{aligned} &\tau < \mu \mathrm{p_c} \quad \text{sticking condition} \\ &\tau = \mu \mathrm{p_c} \quad \text{slipping condition} \end{aligned} \tag{4}$$

Two different values of coefficient of friction were used: $\mu = 0.1$ and 0.4. Figure 8 illustrates the Coulomb's friction model. When the specimen is subjected to remote cyclic loading the crack faces undergo complex contact giving rise to contact pressure and tangential stresses. These stresses, in turn, cause continuous relative sliding or stickslip motion as dictated by the Coulomb's model. A careful analysis of stick-slip motion of the fatigue crack faces gives valuable insight into the mode II behavior of the crack faces. Utilizing Coulomb's friction model in the present study also serves to determine the effect of friction on crack opening levels.

8. Crack opening levels

It is essential to carefully define crack opening levels in mode I and mode II to describe crack closure behavior in slanted and deflected cracks. Most finite element models reported in the past have used the stress at the first node behind crack tip to assess crack opening behavior.

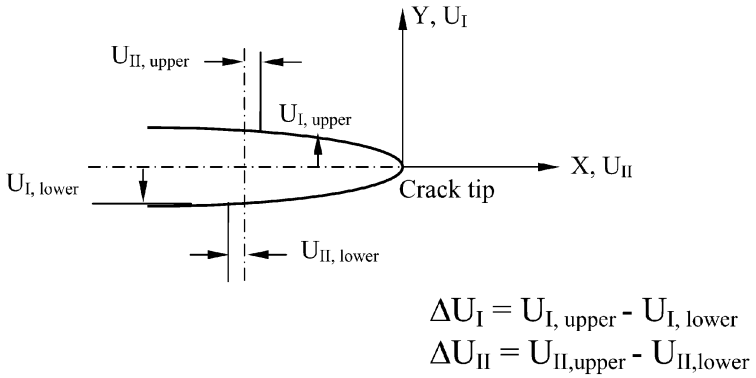

Figure 9. Coordinate system for determining crack flank displacements (based on Smith and Smith, 1988).

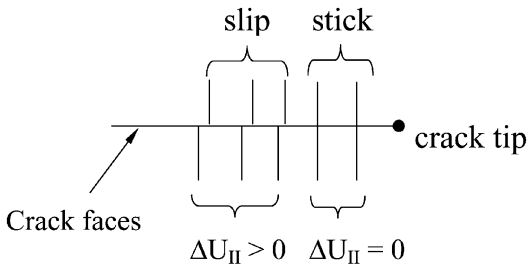

Figure 10. Fatigue crack with partial slip (based on Smith and Smith, 1988).

These include the works of Newman (1976), Ohji and Ogura (1977), Blom and Holm (1985) Fleck (1986), Fleck and Newman (1988), Lalor and Sehitoglu (1988), McClung and Sehitoglu (1989), and Solaki et al. (2003). Some other definitions have also been used: Wu and Ellyin (1996) used the crack tip stress to define crack opening values in mode I by assuming the crack to be fully open when the crack tip stress changes from compressive to tensile. Roychowdhury and Dodds (2003) used the second node behind the crack tip to determine the mode I opening levels. In a recent work, Solanki et al. (2003) monitored the contact stress distribution along the contacting crack faces at minimum load to assess crack opening values. This method however, relies on superposition principle and cannot be valid for large stress levels. Here, we follow the definition which has been employed in most of the previous FE models and define the Mode I crack opening level as the remote stress (denoted by 'S') in a loading cycle at which the normal stress at the first node behind the crack tip changes from compressive to tensile. In the current research, since symmetry has not been employed and both crack faces have been modeled as deformable contact surfaces, it is expected that crack opening displacements in mode I will just change from zero to a positive value (i.e. the crack will be fully open) when the normal stress at the first node behind the crack tip becomes tensile. The elastic-plastic finite element simulations conducted in this study confirm this observation.

The definition of mode II crack opening levels is based on the approach adopted by Smith and Smith (1988). An alternative approach can be based on the concept of sliding mode crack closure (SMCC) first proposed by Tschegg (1983) to explain the reduction in stress intensity at the crack tip of a crack under mode II loading. The concept of SMCC was subsequently used by Brown et al. (1994, 1995) to explain the mode II closure behavior of fatigue cracks. Although, the concept of SMCC is attractive, it is not the most suitable approach for this study. Instead, the concept of 'partial slip' and 'complete slip' put forward by Smith and

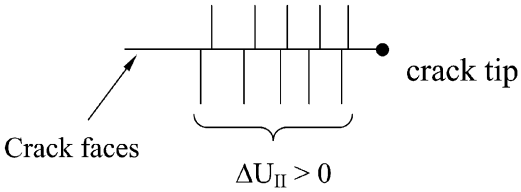

Figure 11. Fully slipped fatigue crack (based on Smith and Smith, 1988).

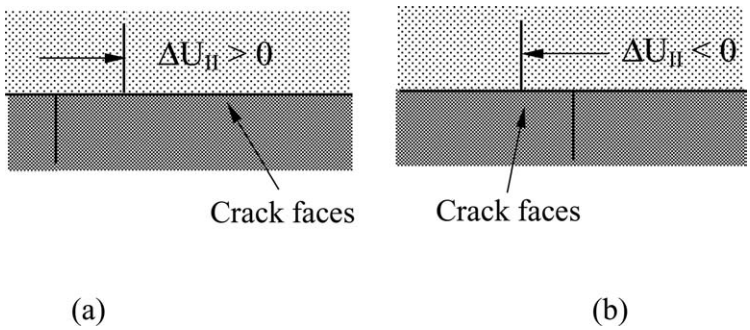

Figure 12. (a) Forward slip (b) Reversed slip (based on Smith and Smith, 1988).

Smith (1988) has been used to describe the crack face interaction in mode II. Figure 9 shows the coordinate system used to determine the crack flank displacements.

Following terms will be used to describe mode II behavior:

1. A crack is said to be 'slipped' at any point along the crack flank, if the mode II displacements are nonzero ($\Delta U_{II} \neq 0$). If the slip has not reached the crack tip then the crack is said to be 'partially slipped' (Figure 10). The crack is said to be 'fully slipped' if the mode II displacements have reached the crack tip as well causing the entire crack to be in slip (Figure 11).
2. If the slip is positive ($\Delta U_{II} > 0$) and occurs during loading portion of the cycle, then the crack is said to be in 'forward slip' (Figure 12a).
3. If the slip is negative ($\Delta U_{II} < 0$) and occurs during unloading portion of the cycle, then the crack is said to be in 'reversed slip' (Figure 12b).
4. If the slip is zero ($\Delta U_{II} = 0$) at all nodes, the crack is said to be 'completely sticking' or simply 'sticking'.
5. The mode II crack opening level is defined as the remote load (denoted by 'S') in the loading portion of the cycle, at which the crack is 'fully slipped'. It should be noted that this slip will be forward slip as per the definition given above. Thus, mode II crack opening level is point of initiation of complete forward slip along the crack flanks.

9. Crack face interaction in a fatigue cycle

Before discussing the results of the finite element simulations, it is pertinent to discuss the important events related to crack closure occurring in a fatigue cycle. Figure 13 shows a schematic of a fatigue cycle. At point A, the crack is subjected to maximum load and experiences maximum crack opening displacement. As the specimen is unloaded, during the first increment of unloading crack tip advances by one or more elements and crack extension is allowed to occur. With further unloading, crack opening displacements gradually reduce,

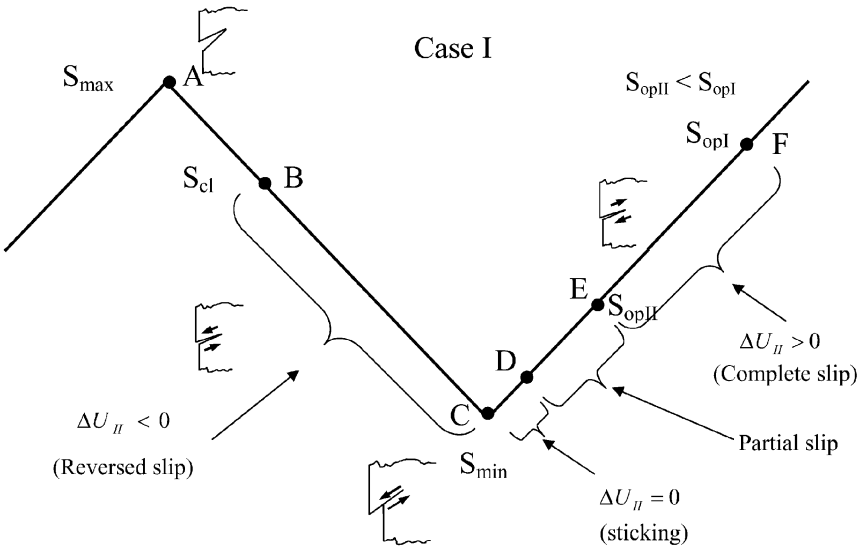

Figure 13. Case I: Crack face interaction in a fatigue cycle -crack slips in mode II before opening in mode I.

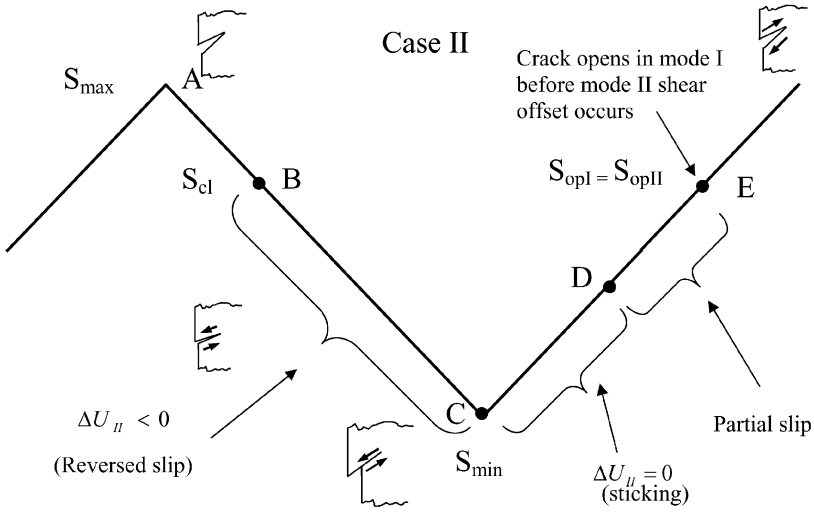

Figure 14. Case II: Crack face interaction in a fatigue cycle – crack faces open in mode I before shear offset in Mode II occurs.

until second (as well as first) node behind the crack tip closes. This event marks the beginning of crack closure and is denoted as B in Figure 13. The applied load at B is the crack closure level denoted by S_{cl}. As the specimen is further unloaded, the crack gradually starts to close. With increasing compressive load the crack faces undergo 'reversed slip' i.e. the upper crack faces slides to the left relative to the lower crack face ($\Delta U_{II} < 0$). At minimum load (point C) in the cycle, the crack faces experience maximum reversed slip.

When is load is increased from minimum, a state of complete stick ($\Delta U_{II} = 0$) is observed till load corresponding to point D is reached. The load range between D to E represents a state of partial slip where slip exits over a part of the crack flanks and has not reached the crack tip yet. Point E represents the load at which slip reaches the crack tip for the first time and complete slip initiates. This load is defined as the mode II opening level in the fatigue cycle.

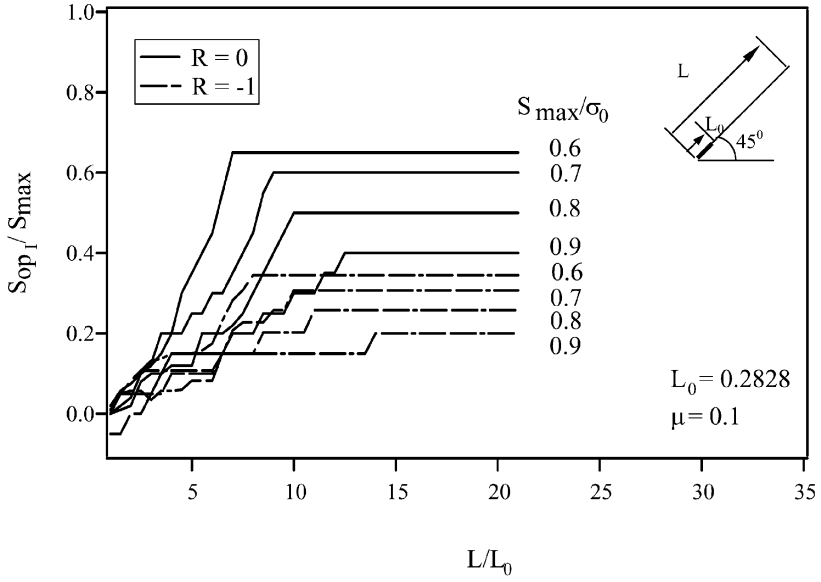

Figure 15. Normalized mode I opening levels for a 45° slanted fatigue crack for two R ratios, Plane stress.

From point E onwards, the crack starts to open in mode I and point F denotes the load at which compressive stresses behind the crack tip change to tensile and the complete crack opens in mode I. This load is defined as mode I crack opening level. It should be noted that Figure 13 depicts the case of 'slip before opening in mode I' i.e. slip propagates to the crack tip before the crack opens completely in mode I. Figure 14 shows the situation in which the crack completely opens in mode I before the crack faces experience mode II shear offset (equivalent to 'positive slip'). This is the case of 'opening in mode I before mode II shear offset'. In this case, mode II opening level is equal to the mode I opening level. Both these cases have been observed in the crack geometries investigated in this research.

10. Finite element results

In the following sections, the results for crack opening behavior based on various finite element analyses have been presented. The effect of following parameters on stable crack opening levels are considered: applied stress level S_{max}/σ_0, load ratio R, crack orientation relative to the applied loading θ, crack path deflection and friction between crack faces. Mode I and mode II crack opening levels for SENT specimens with edge cracks subjected to constant amplitude fatigue loading are examined.

11. Effect of applied stress level and R ratio on crack opening levels

To examine the effect of maximum stress on mode I and mode II opening levels, a SENT specimen with an edge crack oriented at $\theta = 45°$ relative to load direction (geometry 1) was subjected to constant amplitude fatigue loading with four different stress levels S_{max}/σ_0: 0.6, 0.7, 0.8, and 0.9. The dependence of opening levels on R ratio was examined by considering two different values of R: 0 and -1. Figure 15 and Figure 16 show the mode I and mode II crack opening levels respectively, normalized by maximum applied stress in the cycle, as

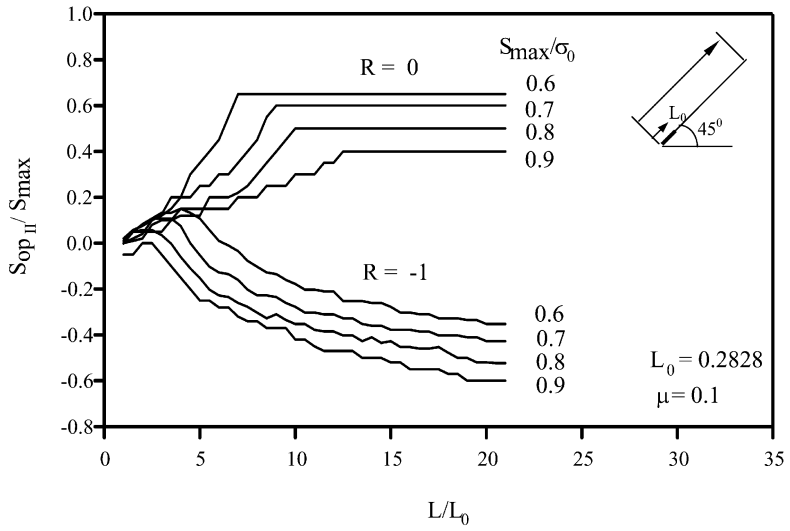

Figure 16. Normalized mode II opening levels for a 45° slanted fatigue crack. For $R = 0$, mode II opening level coincides with mode I opening level (Case II). For $R = -1$, mode II opening occurs before mode I opening (Case I).

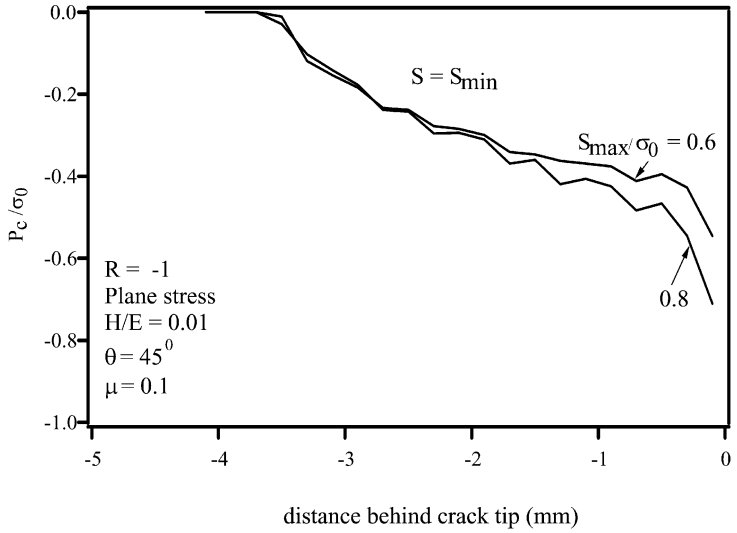

Figure 17. Normalized contact pressure distribution at minimum load in a 45° slanted crack. Pressure distribution at minimum load (and hence resistance to slip) is almost equal for maximum stress levels: 0.6 and 0.8.

a function of normalized crack length. Consider first the mode I opening levels shown in Figure 15. We note that normalized opening stress significantly decrease with increasing maximum stress for both $R = 0$ and $R = -1$. This trend in the stable opening levels has been seen in all numerical and analytical models available in literature. These include the early efforts of Shiratori et al. (1977), Fuhring and Seeger (1979) and Budiansky and Hutchinson (1978). The later works of Newman (1981, 1984), Sehitoglu (1985), Ibrahim et al. (1986), Lalor and Sehitoglu (1986) and McClung and Sehitoglu (1989) confirmed this phenomenon. It should be noted that such dependence of stable opening levels on maximum stress is not obvious. Higher applied stress implies higher inelastic deformation in the wake of the crack and should then

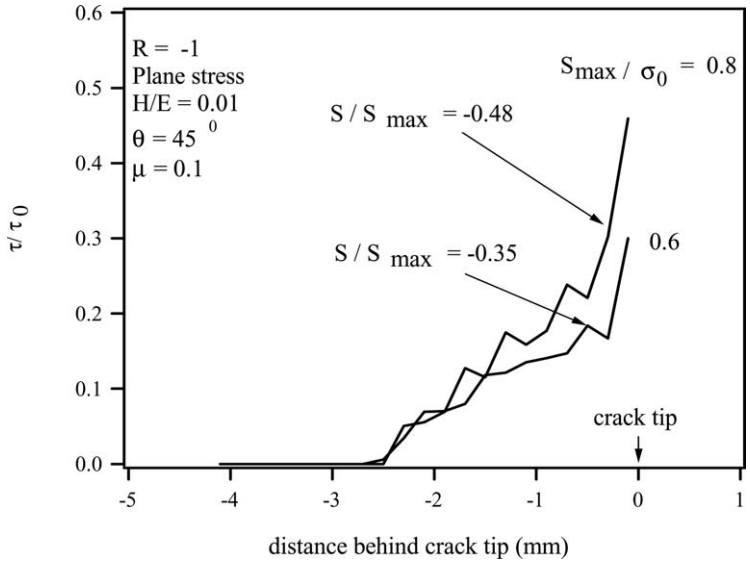

Figure 18. Shear stress distribution along the contacting crack flanks of a 45° slanted crack plotted at remote stress corresponding to mode II opening level (complete slip) for $S_{\max}/\sigma_0 = 0.6$ and 0.8. Although the shear stress distributions are almost identical, the normalized remote stress values, $S/S_{\max}$, producing these distributions are significantly different (-0.35 and -0.48).

result in increased closure- an argument not supported by the results. McClung and Sehitoglu (1989) explained this apparent anomaly by comparing the crack opening displacements of the fatigue crack with that of a 'stationary' crack of the same length subjected to the same maximum stress. This comparison gives a first estimate of residual deformation. The fatigue crack opening is seen as a competition between residual deformation and the 'ideal' crack opening displacement at maximum load. Using this argument, McClung and Sehitoglu (1989) were able to clarify this apparently anomalous behavior. Figure 15 reflects a trend consistent with the above explanation.

Figure 16 shows the mode II opening levels for a 45° slanted crack. First, note a strong dependence of mode II opening levels on the load ratio R. Mode II opening levels continuously increase for $R = 0$ until steady state is attained. On the other hand, for $R = -1$, the mode II opening levels initially increase for small crack lengths, reach a maximum and then, continuously drop before stabilizing. This difference in the nature of the curves for the two load ratios can be explained by a careful examination of the crack face interaction as the crack propagates. For $R = 0$, the crack faces open in mode I before slip reaches the crack tip at any given length of the fatigue crack. This situation is shown in Figure 14 (Case II). The applied mode I load is able to overcome the residual plasticity and open the crack in mode I before the slip state can change from partial slip to complete slip. The crack faces experience shear offset in mode II after mode I opening occurs. This 'opening before shear offset' phenomenon implies that mode II opening level are equal to mode I opening level values for a given crack length. Hence, the mode II opening level curves for $R = 0$ in Figure 16 are identical to the mode I opening level curves in Figure 15. However, mode I and mode II opening level curves are not identical for $R = -1$. This can be explained as follows: during first few cycles, the crack face interaction for $R = -1$ is as depicted in Figure 14, where crack opens in mode I before slip reaches the crack tip. This is the case of 'opening before shear offset' during

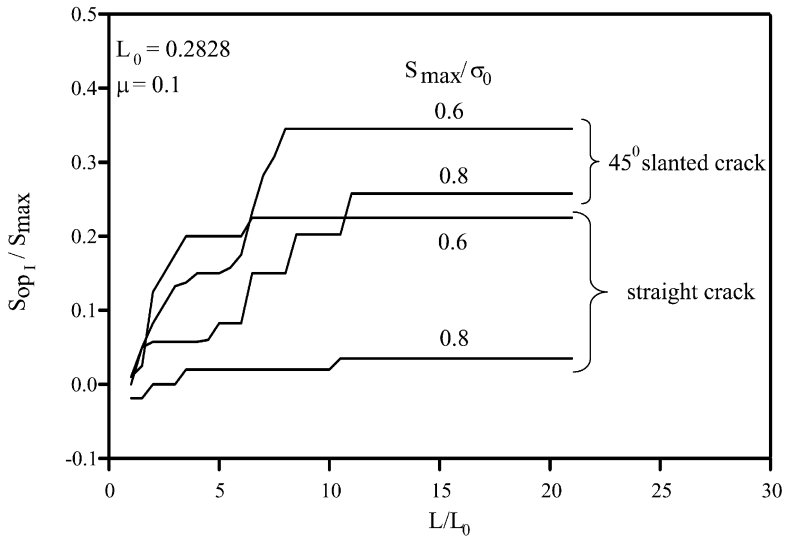

Figure 19. Effect of crack orientation on stable mode I crack opening levels $R = -1$, Plane stress. L_0 is the initial crack length.

which mode II opening levels are equal to mode I opening levels and a monotonic rise in the mode II opening levels is observed. Note that the mode I (and hence mode II) opening levels are essentially low as crack lengths are not large enough to cause substantial forward plastic deformation. Thus, in the case of 'opening before shear offset' phenomenon, mode II opening levels are essentially dictated by mode I opening levels. However, for larger crack lengths, slip reaches the crack tip before the crack opens in mode I. This is the case of 'slip before opening in mode I' (Figure 13). Consequently, mode I and mode II opening levels are no longer equal. With increasing crack length, the event of complete slip initiates at decreasing loads in a fatigue cycle leading to a continuous decrease in the mode II opening loads until steady state is reached.

Another interesting feature of Figure 16 is that stable normalized mode II opening level values decrease with increase in maximum stress S_{max}/σ_0. This trend can be explained on the basis of Coulomb's friction model. The event of complete slip can be seen as a competition between (1) the shear stresses transmitted across the contacting crack faces (which depend on the applied maximum stress) causing the crack faces to slide relative to each other, and (2) the frictional resistance opposing the relative motion which is proportional to the contact pressure distribution along the crack flanks. Figure 17 shows the contact pressure distribution behind the crack tip at minimum load for two stress levels, $S_{max}/\sigma_0 = 0.6$ and 0.8. Note that the normalized contact pressure distribution and hence the frictional resistance does not differ significantly for the two stress levels. Consequently, in accordance with Coulomb's model, shear stress distribution along the crack flank for the two stress levels should be almost identical. Figure 18 confirms this where shear stresses along the crack faces, normalized by the yield stress in shear, are plotted for the two stress levels. These two shear stress distributions correspond to the instant in the fatigue cycle when complete forward slip initiates. Note that although the shear stress distributions are almost identical, the normalized remote stress values, S/S_{max}, producing these distributions are significantly different (-0.35 and -0.48). This implies that mode II crack opening level will be lower at higher maximum stress.

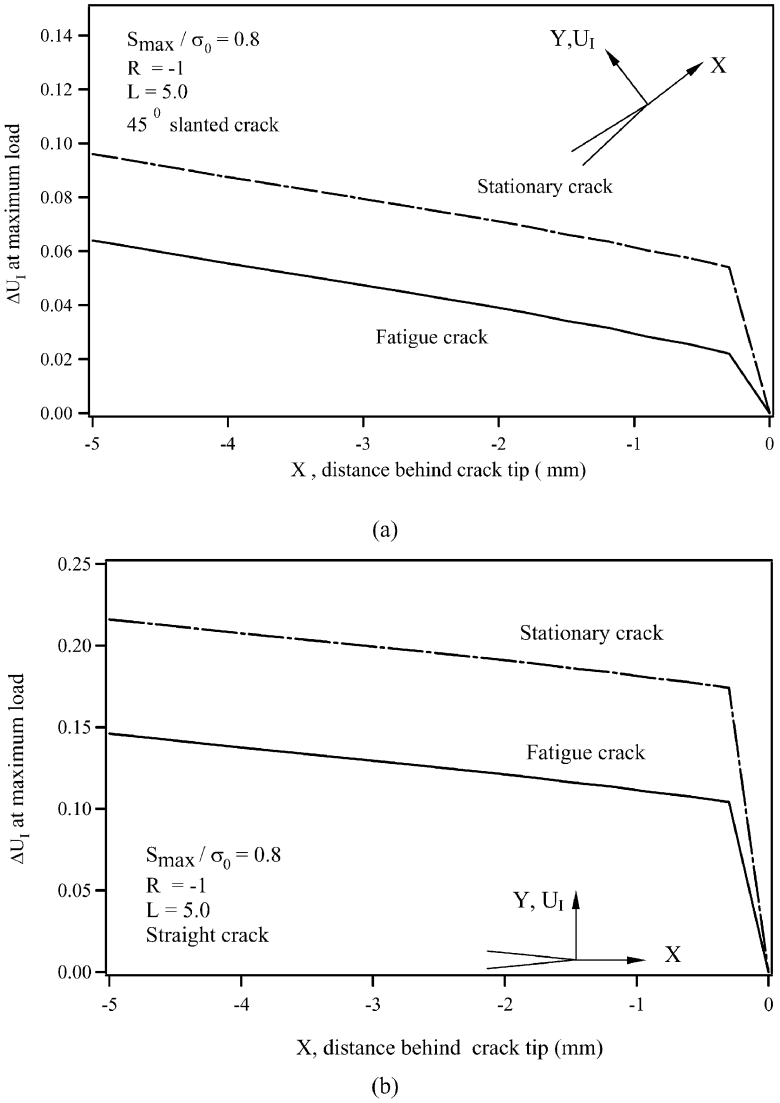

Figure 20. COD at maximum load for (a) 45° lanted crack and (b) straight crack (ΔU_I in mm).

12. Effect of crack orientation

Figure 19 shows the crack opening levels for two crack orientations: a 45° inclined fatigue crack and a straight crack growing in pure mode I. It is seen that stable crack opening level for a 45° slanted crack is significantly higher than that for a straight crack subjected to the same maximum stress. Further, note that the difference in the stable opening level of the two crack geometries increases with increase in maximum stress. Clearly, Figure 19 suggests that an increase in the crack angle will lead to an increase in the mode I crack opening level. Similar findings have been reported in recent past by researchers working on inclined cracks. Wei and James (2002) estimated mode I crack opening levels for crack angles ranging from 0° to 60° for $R = 0.05$. Their results are in agreement with the trend shown in Figure 19. Parry et al.

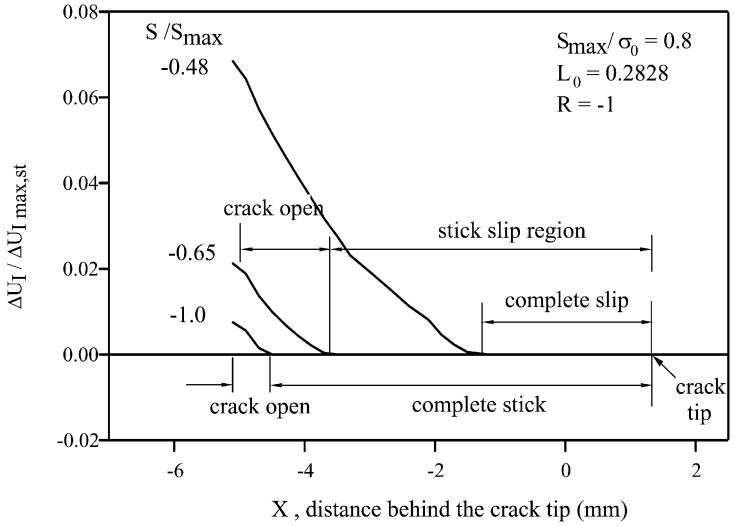

Figure 21a. Normalized mode I displacements at different load levels showing regions of stick, stick-slip and complete slip along the crack flanks (Plane stress).

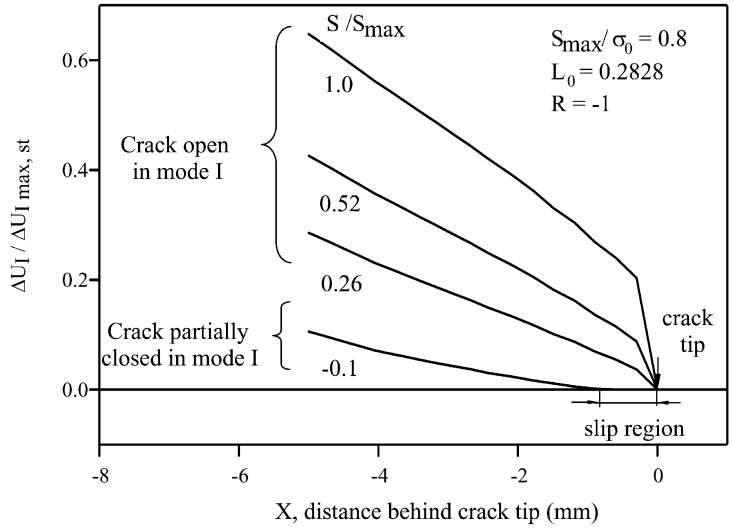

Figure 21b. Normalized mode I displacements at different load levels. Crack tip is shielded at remote load $S/S_{max} = -0.1$. Crack is completely open at all other load levels shown in the plot.

(2000) reported a similar dependence of mode I opening levels on crack angle, although their research focused on both PICC and RICC.

The dependence of S_{op} values on crack angle can be understood by a careful examination of mode I crack opening displacements (ΔU_I) of a straight crack and a 45° inclined crack (Figure 20). The X and Y coordinate axes are respectively parallel and perpendicular to the crack growth direction. The crack opening displacements of both inclined and straight fatigue cracks are compared with CODs of respective stationary cracks of the same length and subjected to the same maximum stress $S_{max}/\sigma_0 = 0.8$, but without any residual deformations in its wake. Figure 20 has several points of interest. First, note the difference in the Y axis scale in Figure 20(a) and 20(b). It is seen that COD of straight crack (fatigue or stationary)

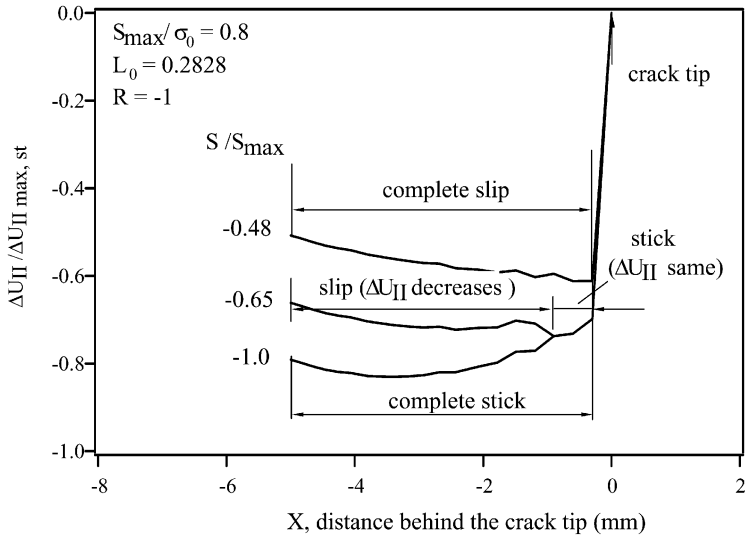

Figure 22a. Normalized mode II COD for a 45° slanted crack at different load levels under plane stress conditions. With increase in remote stress, slip gradually propagates towards the crack tip and reaches the tip at $S/S_{max} = -0.48$.

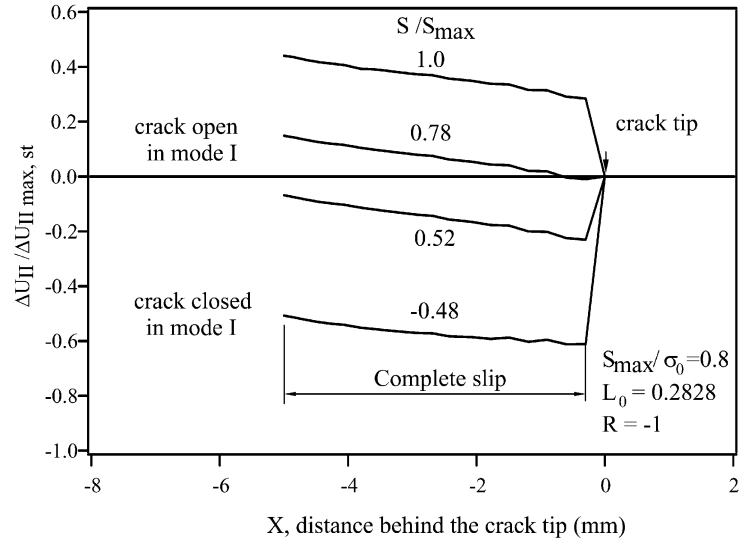

Figure 22b. Normalized mode II COD for a 45° slanted crack at different load levels under plane stress conditions. Mode II displacement does not become positive until the crack completely opens in mode I.

is more than twice that of the 45° inclined crack (fatigue or stationary). This is because in case of the inclined crack, only a fraction of the maximum load is normal to the crack and contributes to mode I COD, while for the straight crack, 100% of applied maximum load contributes to mode I COD. Since the difference in the COD of the fatigue and stationary crack is a measure of the residual deformation δ_{resid}, it is clear that the straight crack has larger residual deformation. As pointed out earlier, crack opening event occurs when the 'ideal' COD (of the stationary crack) at or near the crack tip first exceeds the residual deformation.

In Figure 20(b), the residual deformation for straight crack is a smaller fraction of the total COD, so the opening level for the straight crack will be lower.

13. Crack opening displacement and stress-strain history

The mechanisms which govern plasticity induced crack closure in slanted fatigue cracks bear close relationship with mode I and mode II crack opening displacements as well as the plastic strains at the crack tip. It is therefore, useful to examine the mode I and mode II COD history and stress-strain history at a point ahead of the crack tip along the crack path.

Figure 21 summarizes the mode I crack opening displacements while Figure 22 shows the mode II displacements for $S_{max}/\sigma_0 = 0.8$. In each Figure, Y axis represents the appropriate COD (ΔU_I or ΔU_{II}), normalized by the corresponding COD of a stationary crack at maximum load ($\Delta U_{I\,max,st}$ or $\Delta U_{II\,max,st}$). X axis denotes the distance behind the crack tip corresponding to a fatigue crack length of 5.0. Both mode I and mode II COD values have been determined in accordance with the convention and definition given in Figure 9. Consider the mode I crack opening response (Figure 21). Two plots with two different length scales have been shown, since COD values for compressive loads are very small (note the small length scales in Figure 21(a)). Note that the crack tip is completely shielded at compressive loads (Figure 21(a)) and shielding is observed even at positive stresses as high as $S/S_{max} = 0.13$ (not included in the plot). It is seen that the crack does not open completely in mode I until the normalized applied stress is equal to $S_{opI}/S_{max} = 0.26$ (Figure 21b). However, mode II behavior is significantly different. Consider Figures 22a and 22b which summarize the mode II displacements. Figure 22a shows the progressive propagation of slip towards the crack tip with increase in remote loading. The crack is in 'reversed slip' at minimum load and sticking. As a result, ΔU_{II} values are negative at minimum load. With increase in applied stress, ΔU_{II} values change over part of the crack length ('slip region') and remain unchanged over rest of the crack length (which implies stick). This situation represents a state of 'partial slip' i.e. slip exits over part of the crack only and has not reached the crack tip yet. In Figure 22(a), slip reaches the first node behind the crack tip when $S/S_{max} = -0.48$ and 'complete slip' initiates. As mentioned previously, this load is defined as the mode II crack opening level. Presence of slip along the entire crack flank implies that non-zero mode II stress intensity is developed at the crack tip even though the crack is completely closed in mode I. This result is very important as it implies that a slanted fatigue crack can grow in mode II in spite of remaining closed in mode I. This mode II behavior can significantly affect the crack growth rate predictions and should be taken into account to make reliable fatigue life assessment.

Figure 22b shows the evolution of mode II displacements at loads higher than mode II opening level (-0.48). Notice that the mode II displacements are not necessarily positive for tensile remote loading. For example, it is clear from Figure 22(b) that the crack is fully open in mode I when remote loading becomes $S/S_{max} = 0.52$. But, Figure 22(b) shows that at this remote loading, mode II displacements remain negative over the entire crack flank. In fact, a remote loading equal to 78% of maximum stress is required to change the mode II displacements from negative to positive over the entire crack flank. This mode II behavior can significantly affect the crack growth rate predictions and should be taken into account to make reliable fatigue life assessment.

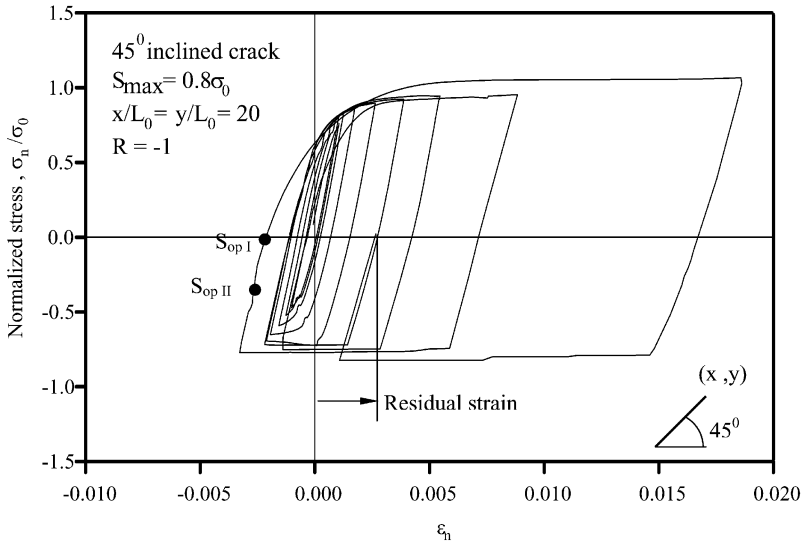

Figure 23. Normal Stress – normal strain history at a material point (x, y) along the inclined fatigue crack as the crack tip approaches and passes it. Plane stress, linear hardening with $H/E = 0.01$.

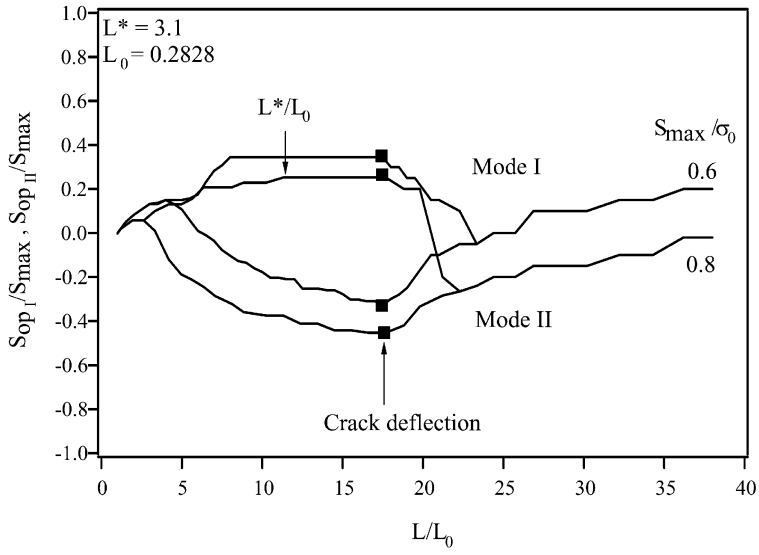

Figure 24. Mode I and II opening levels for a 45° deflected crack. Deflection occurs after stabilization. $R = -1$, Plane stress.

14. Stress-strain history

Figure 23 shows the numerically (FE) simulated stress-strain history at a material point along the 45° inclined crack path as the crack tip approaches it and passes that location. The chosen material point corresponds to a node located at $x/L_0 = y/L_0 = 20$. The plotted stress and strain components are normal to the crack faces and correspond to $R = -1$ and maximum remote stress is $S_{max}/\sigma_0 = 0.8$. Initially, when the crack tip is far from the material point (x, y), the behavior is elastic strain accumulation is not seen. As the crack tip approaches the material point, plastic strain accumulates (the hysterisis loop traverses along x axis to

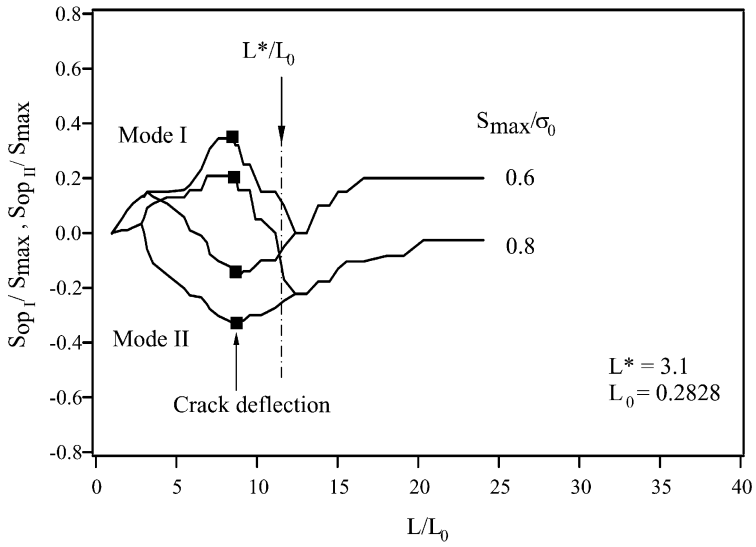

Figure 25. Mode I and II opening levels for a 45° deflected crack. Deflection occurs before stabilization. $R = -1$, Plane stress.

the right). Maximum plastic strain is attained when the crack tip is located at the chosen material point (x, y) and is as high as 1.5%–2%. Once the crack tip passes the material point, strain relaxation occurs, and the strain values drop to about 0.25%. Notice that, once the crack tip passes the material point no further accumulation of strain will occur. In Figure 23, the residual strain in the wake is about 0.25%. The load points at which the crack opens in mode I and mode II (when the crack tip coincides with the material point) are also shown in the figure. Note that crack undergoes complete slip in mode II even though the normal stress σ_n is compressive. When the crack completely opens in mode I, the normal stress *behind* the crack tip is tensile, but, it is compressive *at* the crack tip. Further, note that significant hardening does not occur as the material is cyclically loaded beyond yield. This is expected since the hardening modulus of the material is quite low ($H = 0.01E$). It is also seen that mean stress relaxation does not occur with this (linear hardening) constitutive model. As pointed out by McClung and Sehitoglu (1989), this phenomenon of absence of stress relaxation has significant influence on the crack advance scheme. If the specimen is subjected to two full cycles of loading before advancing the crack by one or more elements, local stress redistribution will occur. However, for linear hardening, mean stress will not relax, and the stress-strain response will becomes stable resulting in stable opening levels. The simplicity and stability of the stress-strain behavior in a bilinear model makes it an attractive choice for constitutive modeling.

15. Effect of crack deflection

Another important factor influencing the closure behavior of a fatigue crack is crack path deflection. Figure 15 summarizes the stable mode I opening levels for a 45° slanted crack which is allowed to propagate along the initial orientation without deflection. However, a fatigue crack propagating in mixed-mode will tend to deflect in order to grow along the preferred plane or direction. It is therefore, reasonable to expect that the 45° slanted crack

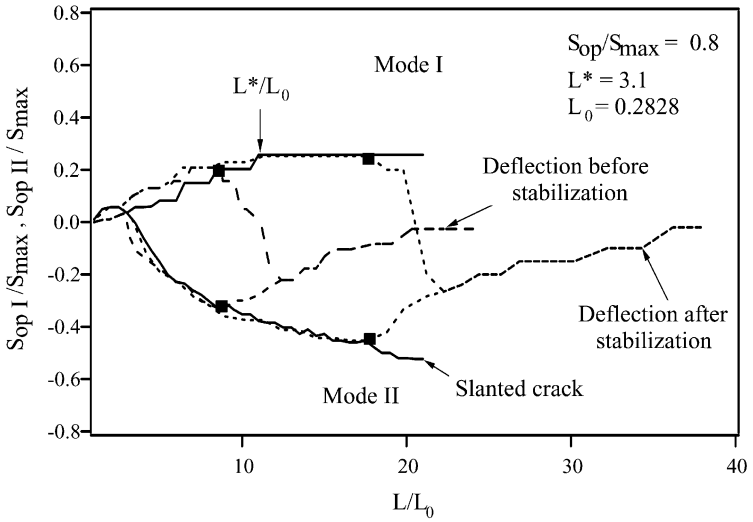

Figure 26. Comparison of opening levels for slanted and deflected fatigue cracks.

considered in the previous sections will, at some point, deflect from its initial orientation and start growing in pure mode I. Here, we investigate the effect of such a deflection.

Note from Figure 15 that mode I opening levels attain a steady state at different fatigue crack lengths depending on the maximum stress and *R* ratio. Further, for a given *R* ratio, the crack length required to achieve stable opening levels increases with increase in maximum stress. This phenomenon brings out the following two possible cases of crack deflection:

1. Occurrence of crack deflection after mode I opening levels attain stabilization.
2. Occurrence of crack deflection before mode I opening levels attain stabilization.

In order to investigate the above two cases, it is essential to establish a measure of minimum slanted crack length, denoted by L^*, required for stabilization. A logical definition of L^* is the transition crack length corresponding to the highest maximum stress, S_{max}/σ_0, used to simulate crack deflection. In deflected crack simulations, two stress levels were considered: $S_{max}/\sigma_0 = 0.6$ and 0.8. The transition crack length for $S_{max}/\sigma_0 = 0.8$ is 3.1 and is assigned to L^*. The normalized minimum transition length is given by $L^*/L_0 = 11$. Figures 24 and 25 show the mode I and mode II opening levels as a function of crack length. Consider Figure 24 which depicts the case of 'deflection after stabilization' (Geometry 2 in Figure 3). First, note the steep decrease in the mode I opening levels immediately after deflection, while a gradual rise in mode II opening levels occurs at the same time. The increase in mode II opening levels is primarily due to increased resistance to slip offered by the straight portion of the fatigue crack. Note that mode I opening level decreases until it equals mode II S_{op}. The point of equalization of mode I and mode II opening levels represents the crack length at which the phenomenon of crack face interaction changes from 'slip before opening' to 'opening before shear offset'. In other words, for smaller lengths of the straight crack, the entire crack slips before opening in mode I. However, when the length of the straight portion becomes comparable to the inclined portion of the fatigue crack, frictional resistance is too high to permit complete slip. Hence, the crack opens completely in mode I before mode II shear offset occurs. Comparison of Figure 24 (and Figure 25) with Figure 19 reveals that the final opening levels values of the deflected fatigue crack are very close to the opening levels of a pure mode I straight crack subjected to the same maximum stress. This implies that once the

length of the straight portion becomes very large, the deflected crack behaves as a pure mode I straight crack and the slanted portion of the crack will no longer play any role in determining the mode I opening levels. For such a crack, mode II component will be nonexistent. However, it is not clear from Figure 24 if the stable opening level values have been reached for the straight portion of the crack. We note that the above lack of stabilization in Figure 24 appears to arise out of the delayed deflection of the crack front. It is possible that the opening levels will continue to increase by a small amount for a few more cycles before stabilization occurs. It is, however, reasonable to expect that the final stable opening level value will be close to the stable opening levels of pure mode I straight crack (refer to Figure 19).A similar trend is seen in Figure 25 which depicts the case of 'deflection before stabilization' (Geometry 3 in Figure 3). Crack deflection results in an immediate drop in the mode I opening levels and an increase in the mode II opening levels until the two opening level values become equal. As pointed out earlier, this equality represents a change in the crack face interaction from 'slip before opening' to 'opening before shear offset'. With further increase in the length of the straight portion, opening levels rise steadily and attain stable values. These stable opening level values are in close agreement with the stable opening levels of pure mode I straight crack (refer to Figure 19). Thus, it appears that deflection of crack before or after stabilization of mode I opening levels will not significantly affect the final stable opening level values. What then can be learned from these two cases of crack deflection? To identify significant points of interest, consider Figure 26 which compares the mode I and mode II opening levels of the two deflected crack cases with those of a 45° slanted crack for $S_{max}/\sigma_0 = 0.8$. Note that the mode I and mode II opening level curves for the slanted crack do not coincide exactly in the three simulations. This is because three different finite element meshes were used to examine these three cases. However, the predicted opening level variations for the slanted portion of the crack, using the three different finite element meshes, do not differ significantly. This implies that the results are free of mesh size effects.

Notice that crack growth rate will accelerate after crack deflection since mode I opening levels drop steeply in both the cases of crack deflection. However, crack growth acceleration will be higher in case of 'deflection after stabilization' since, the crack experiences higher effective stress intensity for this case. Also, note that in this case, the crack continues to experience lower mode I opening stresses (hence higher effective stress intensity) for almost all crack lengths. This implies that the crack growth rates will be the highest for geometry 2 ('deflection after stabilization') once the crack deflects towards the preferred plane of growth.

16. Effect of friction

It is clear from previous sections that closure behavior of a slanted fatigue crack is significantly affected by crack face interaction which in turn, is dependent on the extent of surface roughness of the crack faces. The roughness of the crack faces can be modeled at two levels: micro and macro. Cracks growing in near threshold regime in planar slip materials and coarse-grained materials are likely to have micro-level non-flat surfaces and the growth behavior of such cracks is influenced by the contact interaction and relative sliding between faces. Micro-level roughness of crack faces can be done using Gaussian or other types of distribution of asperity heights (e.g.: Garcia and Sehitoglu, 1995). In this research, the roughness of the crack faces has been modeled at macro-level using Coulomb's friction model. The coefficient of friction, μ, can be treated as a preliminary measure of roughness of crack faces. It is then

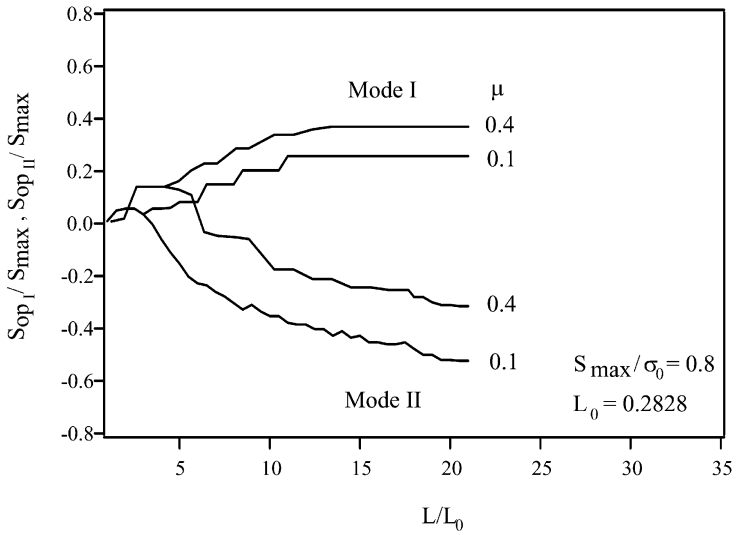

Figure 27. The role of friction coefficient on opening levels for a 45° slanted crack, Plane stress, $R = -1$. Results show that for low friction coefficient, the crack opening stresses are lower.

possible to investigate the effect of friction on crack closure by considering different values of μ. Figure 27 shows the mode I and mode II opening levels for a slanted cracks subjected to maximum stress $S_{max}/\sigma_0 = 0.8$ and two different values of friction coefficient μ: 0.1 and 0.4.

For smaller crack lengths, increase in μ has no significant effect on either mode I or mode II opening level. However, for $\mu = 0.4$, separation of the mode I and mode II S_{op} curves occurs at a larger crack length value. Note also that the final stable opening levels are higher for $\mu = 0.4$. The increase in mode II opening levels is rather expected: increased friction will offer greater resistance to relative sliding between the crack faces, thus requiring higher applied stress to produce complete slip along the crack flanks. Mode I opening, on the other hand, is primarily dependent on the crack tip displacements and the residual deformation in the wake of the crack. However, Figure 27 suggests a secondary dependence of mode I opening on friction between the crack faces. Similar dependence of mode I opening stress on friction coefficient has been reported by Wei and James (2002). Thus, it is seen that increased friction will lead to increase in mode I and mode II opening levels.

17. Discussion

The finite element results highlight significant differences in the closure behavior of slanted/deflected cracks when compared to straight cracks. First, note that both mode I and mode II components are seen in slanted/deflected cracks, while, mode II behavior is absent in straight cracks subjected to remote mode I loading. Finite element results reveal that mode I crack opening levels of slanted cracks are significantly higher than the opening levels of straight cracks. Consequently, crack growth rates for non-planar cracks cannot be realistically estimated from calculations based on straight cracks.

It is also essential to consider the effect of mode II component on crack growth rates of slanted cracks. Depending on the R ratio, a slanted crack may exhibit potential to propagate in mode II while still being closed in mode I. For negative R ratios, a slanted crack is likely to undergo complete slip in mode II before opening in mode I. In such cases, crack growth is

possible in mode II when the crack is closed in mode I. However, for positive R ratios, crack opening in mode I occurs before mode II displacements can reach the crack tip. In this case, crack growth will essentially occur only after crack opens in mode I.

Finally, it is clear that mode I crack opening levels depend not only on the residual plasticity in the wake but also on friction between the crack faces. This secondary dependence of mode I crack opening level on friction was not apparent in previous finite element studies, since, almost all of the previous models used symmetry and failed to include crack face interactions and the resulting frictional effects in their models.

18. Conclusions

1. Crack opening stresses (normalized by maximum stress) for a 45° slanted fatigue crack are found to be significantly higher than the normalized values for a straight crack. This indicates a clear dependence of closure behavior on crack orientation.
2. The mode I opening levels of a 45° inclined crack increase to a stable value with increase in crack length. However, variation of mode II opening levels with crack length is a function of R ratio. For $R = 0$, mode II crack opening stresses follow the same trend as mode I opening levels. For $R = -1$, the mode II opening levels initially increase for small crack lengths and then steadily decrease before finally stabilizing.
3. The normalized stable mode I and mode II opening levels are a function of both R ratio and far-field maximum stress. The stable opening level values are higher for higher R ratios. For a given R ratio, both mode I and mode II opening levels decrease with increase in far-field maximum stress.
4. Two fundamental types of mode II crack face interactions are identified: (a) 'slip before opening' where the crack faces completely slip in mode II before opening in mode I and, (b) 'opening before shear offset' where the crack faces open in mode I before suffering lateral displacements in mode II. 'Slip before opening' type of interaction is dominant for $R = -1$, while, 'opening before shear offset' type of crack face interaction dominates for $R = 0$.
5. Deflection of a 45° slanted crack from its initial orientation to pure mode I results in an immediate drop in the mode I opening levels and an increase in the mode II opening levels until the two opening level values become equal. Subsequent to the point of equality, an increase in the crack length results in an increase in mode I (and mode II) opening stress to a stable value.
6. The final normalized crack opening stress for a deflected crack is very close to the stable opening stress of a straight crack. This indicates that when the length of the straight portion of the fatigue crack becomes comparable to the slanted crack length, the deflected crack behaves as a pure mode I straight crack and the slanted portion of the crack will no longer play any role in determining the mode I opening levels.
7. Deflection of a slanted crack can occur before or after the slanted-crack mode I opening level achieves stable value. However, the final opening stresses for the two deflected crack configurations are equal. In other words, the point of deflection will not affect the final stable crack opening stress of the deflected crack.
8. Stable mode I and mode II opening stresses for a slanted crack depend on the coefficient of friction between the crack faces. Increase in the friction coefficient results in increase in stable opening stresses.

Acknowledgements

This research was financially supported by Federal Railroad Administration (FRA). The computational support was provided by National Center for Supercomputing Applications (NCSA), UIUC. All finite element simulations were carried out on Origin 2000 supercomputers at NCSA, University of Illinois.

References

ABAQUS/ Standard User's Manual, version 6.1, HKS, 2000

Alwar, R.S. and Thiagarajan, S. (1986). Effect of crack closure on crack initiation parameters. *Engineering Fracture Mechanics* **25**(1), 23–29.

Blom, A. and Holm, D.K. (1985). An experimental and numerical study of crack closure. *Engineering Fracture Mechanics* **22**, 997–1011.

Budiansky, B. and Hutchinson, J.W. (1978). Analysis of closure in fatigue crack growth. *J. Applied Mechanics, Trans. ASME* **45**, 267–276.

Carlson, R.L. and Beevers, C.J. (1985). A mixed mode fatigue crack closure model. *Engineering Fracture Mechanics* **22**(4), 651–660.

Chermahini, R.G., Shivkumar, K.N. and Newman, J.C., Jr. (1988). Three-dimensional finite-element simulation of fatigue crack growth and closure. *ASTM STP 982* 398–413.

Comninou, M. and Dundurs, J. (1979). On frictional contact in crack analysis. *Engineering Fracture Mechanics* **12**, 117–123.

Elber, W. (1971). Damage tolerance in aircraft structures. *ASTM STP 486* 230–242.

Elber, W. (1970). Fatigue crack closure in cyclic tension. *Engineering Fracture Mechanics* **2**, 37–45.

Fleck, N.A. (1986). Finite element analysis of plasticity induced crack closure under plane strain conditions. *Engineering Fracture Mechanics* **25**, 441–449.

Fleck, N.A. and Newman, J.C., Jr. (1988). Analysis of crack closure under plane strain conditions. *ASTM STP 982* 319–341.

Forsyth, P.J.E. (1963). Fatigue damage and crack growth in aluminum alloys. *Proceedings of Mechanisms Of Fatigue In Crystalline Solids, Acta Metallurgica* **11**, 703–715.

Fuhring, H. and Seeger, T. (1979). Dugdale closure analysis of fatigue cracks under constant amplitude loading. *Engineering Fracture Mechanics* **11**, 99–122.

Gall, K., Sehitoglu, H. and Kadioglu, Y. (1996). FEM study of fatigue crack closure under double slip. *Acta Materiala* **44**(10), 3955–3965.

Ibrahim, F.K., Thompson, J.C. and Topper, T.H. (1986). A study of the effect of mechanical variables on fatigue crack closure and propagation. *International Journal of Fatigue* **8**(3), 135–142.

Lalor, P. and Sehitoglu, H. (1988). Crack closure outside small scale yielding regime. *ASTM STP 982* 342–360.

Llorca, J. (1992). Roughness induced fatigue crack closure: A numerical study. *Fatigue and Fracture of Engineering Materials and Structures* **15**(7), 655–669.

McClung, R.C. and Sehitoglu, H. (1989). Finite element analysis of fatigue crack closure 1. Basic modeling issues. *Engineering Fracture Mechanics* **33**(2), 237–252

McClung, R.C. and Sehitoglu, H. (1989). Finite element analysis of fatigue crack closure 2. Numerical results. *Engineering Fracture Mechanics* **33**(2), 253–272.

Mendelsohn, D.A. and Wang, K.H. (1988). Partial release and relocking of a frictionally locked crack due to moving tensile loads. *Journal of Applied Mechanics* **55**, 383–388.

Nakagaki, M. and Atluri, S.N. (1980). Elastic-plastic analysis of fatigue crack closure modes I and II. *AIAA Journal* **18**(9), 1110–1117.

Nakagaki, M. and Atluri, S.N. (1979). Fatigue crack closure and delay effects under mode I spectrum loading: An effect elastic-plastic procedure. *Fatigue of Engineering Materials and Structures* **1**, 421–429.

Nakamura, H., Kobayashi, H., Yanase, S. and Nakazawa, H. (1983). Finite element analysis of fatigue crack closure in compact specimen. *Mechanical Behavior of Materials*, Fourth Int. Conf. Mechanical Behavior of Materials, Stockholm, Aug., Pergamon, **2**, 817–823.

Newman, J.C., Jr. (1981). A crack-closure model for predicting fatigue crack growth under aircraft spectrum loading. *ASTM STP 748*, 55–84.

Newman, J.C., Jr. (1984). A crack-opening stress equation for fatigue crack growth. *International Journal of Fracture* **24**, R131–R135.

Newman, J.C., Jr. (1976). Finite element analysis of crack growth under monotonic and cyclic loading. *ASTM STP 590* 284–301.

Newman, J.C., Jr. and Arman, H., Jr. (1975). Elastic-plastic analysis of a propagating crack under cyclic loading. *AIAA Journal* **13**(8), 1017–1023.

Ohji, K. and Ogura, K. (1977). FEM analysis of crack closure and delay effects in fatigue crack growth under variable amplitude loading. *Engineering Fracture Mechanics* **9**(2), 471–480.

Ohji, K., Ogura, K. and Okhubo, Y. (1974). On the closure of fatigue cracks under cyclic tensile loading. *Internaitonal Journal of Fracture* **10**, 123–124.

Parry, M.R., Syngellakis, S. and Sinclair, I. (2000). Numerical modeling of combined roughness and plasticity induced crack closure effects in fatigue. *Material Science and Engineering* **A291**, 224–234.

Qian, J. and Fatemi, A. (1996). Mixed mode fatigue crack growth: A literature survey. *Engineering Fracture Mechanics* **55**, 969–990.

Roychowdhury, S. and Dodds, R.H., Jr. Three-dimensional effects on fatigue crack closure in the small scale-yielding regime. *Fatigue and Fracture of Engineering Materials and Structures*, submitted for publication.

Sehitoglu, H. and Sun, W. (1990). Modeling of plane strain fatigue crack closure. *ASME Journal of Engineering Materials and Technology* **113**, 31–40.

Sehitoglu, H. and Sun, W. (1992). Residual stress fields during fatigue crack growth. *Fatigue and Fracture of Engineering Materials and Structures* **15**(2), 31–40.

Sehitoglu, H. (1985). Crack opening and closure in fatigue. *Engineering Fracture Mechanics* **21**(2), 329–339.

Sehitoglu, H. and Garcia, A. (1997). Contact of crack surfaces during fatigue: Part 1. Formulation of the model. *Metallurgical and Materials Transactions A* **28A**, 2263–2275.

Sehitoglu, H. and Garcia, A. (1997). Contact of crack surfaces during fatigue: Part 2. Simulations. *Metallurgical and Materials Transactions A* **28A**, 2277–2289.

Shiratori, M., Miyoshi, T., Miyamoto, H. and Mori, T. (1977). A computer simulation of fatigue crack propagation based on the crack closure concept. *Adv. In Research on the Strength and Fracture of Materials (Fracture 1977)*, Fourth Int. Conf. Fracture, Waterloo, Canada, Pergamon, **2B**, 1091–1098.

Smith, M.C. and Smith, R.A. (1988). Towards an understanding of mode II fatigue crack growth. *ASTM STP 924* 260–280.

Solanki, K., Daniewicz, S.R. and Newman, J.C., Jr. A new methodology for computing crack opening values from finite element analyses. *Engineering Fracture Mechanics*, submitted for publication.

Solanki, K., Daniewicz, S.R. and Newman, J.C., Jr. (2003). Finite element modeling of plasticity-induced crack closure with emphasis on geometry and mesh refinement effects. *Engineering Fracture Mechanics* **70**, 1475–1489.

Suresh, S. and Ritchie, R. (1982). A geometric model for fatigue crack closure induced by fracture surface roughness. *Metallurgical Transactions A* **13A**, 1627–1631.

Tong, J., Brown, M.W. and Yates, J.R. (1995). A model for sliding mode crack closure. Part I: Theory for pure mode II loading. *Engineering Fracture Mechanics* **52**(4), 599–611.

Tong, J., Brown, M.W. and Yates, J.R. (1995). A model for sliding mode crack closure. Part II: Mixed mode I and II loading and application. *Engineering Fracture Mechanics* **52**(4), 613–623.

Tong, J., Yates, J.R. and Brown, M.W. (1992). The significance of mean stress effects on the fatigue crack growth threshold under mixed mode I/II loading. *Fatigue Frac. Engng. Mater. Struct.* **17**, 829–838.

Tschegg, E.K, Ritchie, R.O. and McCintock, F.A. (1983). On the influence of rubbing fracture surfaces on fatigue crack propagation in mode III. *International Journal of Fatigue* **28**, 29–35.

Tschegg, E.K. (1983). Sliding mode crack closure and mode III fatigue crack growth in mild steel. *Acta Metallurgica* **31**(9), 1323–1330.

Wei, L. and James, M.N. (2002). Fatigue crack closure of inclined and kinked cracks. *International Journal of Fracture* **116**, 25–50.

Wu, J. and Ellyin, F. (1996). A study of fatigue crack closure by elastic-plastic finite element analysis for constant-amplitude loading. *International Journal of Fracture* **82**, 43–65.